BIOCHEMISTRY
including biophysical chemistry & molecular biology

Article

pubs.acs.org/biochemistry

Structural and Functional Implications of the Yeast High-Affinity Tryptophan Permease Tat2

Naoko Kanda[†] and Fumiyoshi Abe*[,†,‡]

[†]Department of Chemistry and Biological Science, College of Science and Engineering, Aoyama Gakuin University, Sagamihara, Japan
[‡]Institute of Biogeosciences, Japan Agency for Marine-Earth Science and Technology (JAMSTEC), Yokosuka, Japan

ABSTRACT: Tryptophan is hydrophobic, bulky, and the rarest amino acid found in nutrients. Accordingly, the import machinery can be specialized evolutionarily. Our previous study in *Saccharomyces cerevisiae* demonstrated that tryptophan import by the high-affinity tryptophan permease Tat2 is accompanied by a large volume increase during substrate import. Nevertheless, the mechanisms by which the permease mediates tryptophan recognition and permeation remain to be elucidated. Here we determined amino acid residues essential for Tat2-mediated tryptophan import. By means of random mutagenesis in combination with site-directed mutagenesis based on crystallographic studies of the *Escherichia coli* arginine/agmatine antiporter AdiC, we identified 15 amino acid residues in the Tat2 transmembrane domains (TMDs) 1, −3, −5, −8, and −10, which are responsible for tryptophan uptake. T98, Y167, and E286 were assumed to form the central cavity in Tat2. G97/T98 and E286 were located within the putative α-helix break in TMD1 and TMD6, respectively, which are highly conserved among yeast amino acid permeases and bacterial solute transporters. Given the conformational change in AdiC upon substrate binding, G97/T98 and E286 of Tat2 were assumed to mediate a structural shift from an outward-open to a tryptophan-bound-occluded structure upon tryptophan binding, and T320, V322, and F324 became stabilized in TMD7. Such dynamic structural changes may account for the large volume increase associated with tryptophan import occurring concomitantly with a movement of water molecules from the tryptophan binding site. We also propose the working hypothesis that E286 mediates the proton influx that is coupled to tryptophan import.

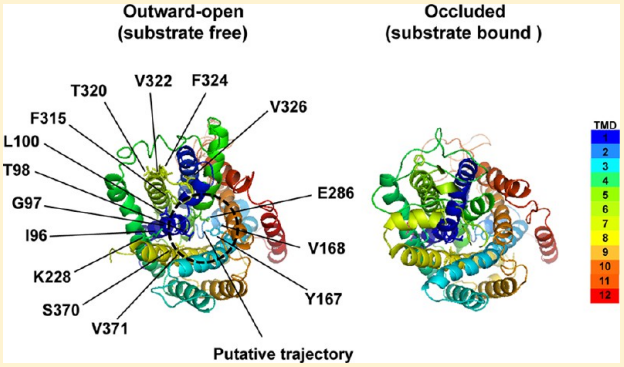

INTRODUCTION

Tryptophan is hydrophobic, bulky, and the rarest amino acid found in nutrients and nature. This leads to the concept that the tryptophan uptake machinery can be evolutionarily specialized in heterotrophic organisms. Tryptophan is an essential amino acid for animals including humans. It functions as a biochemical precursor of the neurotransmitter serotonin, the brain hormone melatonin, or the phytohormone auxin and contributes to the synthesis of the coenzymes NADH and NADPH via the kynurenine pathway.[1−4] In rats, the T-type amino acid transporter-1 TAT1 (also known as MCT10 or *SLC16A10*, TCOD# 2.A.1.13.2), which is strongly expressed in the intestine, placenta, and liver, mediates the import and export of aromatic amino acids in a proton- and sodium-independent manner.[5] When TAT1 is expressed in *Xenopus* oocytes for import assay, the K_m values for tryptophan, phenylalanine, and tyrosine are 3.72, 7.02, and 2.59 mM, respectively.[5] TAT1 belongs to the monocarboxylate transporter family that consists of 14 members with different substrate specificities, types of coupling ions, and tissue distribution.[6]

The family of amino acid permeases in the yeast *Saccharomyces cerevisiae* comprises 24 members, which all exhibit a nearly identical membrane topology with 12 putative transmembrane domains (TMDs) and cytoplasmic tails except for Ssy1, a subunit of the SPS amino acid sensor complex.[7,8] It is the second-largest family of the yeast major facilitator superfamily proteins.[7,9] Amino acid transport in yeast is coupled to the proton motive force generated by the plasma membrane H^+-ATPase Pma1.[9] The molecular mechanism by which any amino acid residue mediates H^+/substrate coupling is unknown. Tryptophan is imported through the function of Tat1 and Tat2, which are the low-affinity and high-affinity tryptophan permeases in *S. cerevisiae*, respectively. *TAT1* and *TAT2* were originally identified as genes conferring resistance to the immunosuppressive agent FK506.[10,11] Because tryptophan uptake is highly sensitive to diverse environmental stresses, it becomes the limiting factor for cell growth in tryptophan-auxotrophic strains. Of the two permeases, Tat2 has been relatively well characterized in terms of ubiquitin-dependent degradation and intracellular trafficking. In response to nutrient deprivation, rapamycin treatment or cycloheximide treatment, Tat2 undergoes ubiquitination in a manner dependent on Rsp5 ubiquitin ligase and arrestin-related trafficking adaptors, followed by vacuolar degradation.[12−14] Although intracellular trafficking and ubiquitin-mediated regulation have been well documented in

Received: April 14, 2013
Revised: June 1, 2013
Published: June 4, 2013

   dx.doi.org/10.1021/bi4004638 | *Biochemistry* 2013, 52, 4296−4307

Tat2, the structure and mechanism of tryptophan import are still unclear.

We demonstrated that tryptophan uptake by *S. cerevisiae* cells is highly sensitive to high hydrostatic pressure. When cells of tryptophan-auxotrophic strains are exposed to pressure of 25 MPa (approximately 250 kg cm^{-2}) for more than 5 h, the cell cycle is arrested in the G_1 phase.[15] Under this condition, Tat2 is degraded in an Rsp5-dependent manner.[16−18] The effects of hydrostatic pressure on an enzymatic reaction are interpreted within the framework of the simplest kinetic mechanism in which the transition state presents the highest energy barrier, and the chemical transformation of substrate to product is considered to be a single rate-limiting step.[19−21] Assuming that tryptophan is imported based on this simplest model, we determined the activation volume ($\Delta V‡$) for Tat1- and Tat2-mediated tryptophan import. $\Delta V‡$ represents the volume difference between the basal state and the transition state. The large $\Delta V‡$ for Tat1- and Tat2-mediated tryptophan import (89.3 mL mol^{-1} and 50.8 mL mol^{-1}, respectively) suggests that these permease proteins undergo a dramatic structural expansion by increasing internal cavities upon tryptophan import or by breaking certain internal interactions to bind tryptophan, or that tryptophan binding and closure of the proteins releases water of solvation of Tat1/Tat2 and tryptophan, which has a larger volume in the bulk solvent than when the water molecules are bound to the proteins and tryptophan. Nevertheless, amino acid residues responsible for the conformational change or substrate recognition and specificity are completely unknown in both Tat1 and Tat2.

Crystallographic information on homologous proteins allows us to elucidate the mechanisms of substrate import through structurally unknown permeases using a rational mutational analysis of conserved residues. The AdiC antiporter in *Escherichia coli* and other enteric bacteria prevents internal acidification in extremely acidic environments by exchanging L-arginine (Arg^+) for intracellular agmatine (Agm^{2+}).[22−24] AdiC belongs to the amino acid-, polyamine-, and organic cation-superfamily of transporters, and is the closest structural paradigm for Tat2 among structurally determined transporters. The crystal structure of AdiC has been determined at a high resolution.[25−27] Mechanistically, the AdiC structures of the wild-type and the N22A-L123W mutant represent two conformational states within the transport cycles: the outward-open (PDB: 3LRB and 3NCY) and the outward-facing Arg^+-bound occluded (PDB: 3L1L), respectively.[25,27] Although AdiC is structurally the closest to Tat2 among the transporters registered in the RSCB protein databank, they are only distantly related, with amino acid identity of 21% and similarity of 39% in the protein−protein BLAST search (http://blast.ncbi.nlm.nih.gov/). Thus, the molecular understanding of tryptophan import by Tat2 remains hampered by the lack of transporters with tryptophan specificity for which the structure has been resolved.

In the present study, we determined critical amino acid residues for Tat2-mediated tryptophan import by means of random mutagenesis using error-prone PCR in combination with site-directed mutagenesis based on AdiC crystal structures and demonstrate that a putative tryptophan-binding pocket is surrounded by some of the critical amino acid residues in Tat2. We assume that E286 in TMD6, a highly conserved glutamate in the yeast amino acid permeases and bacterial transporters, plays a central role in putative conformational shifts of Tat2 upon tryptophan binding, and E286 might mediate the symport of protons. In addition to the important amino acid residues in TMD1, −3, −6, and −8 primarily involved in the putative conformational shifts of Tat2, the role of residues located on the peripheral side of TMD7 is also described.

MATERIALS AND METHODS

Yeast Strains and Culture Conditions. The parental wild-type strain YPH499 (*MAT***a** *ura3−52 lys2−801 ade2−101 trp1-Δ63 his3-Δ200 leu2-Δ1*) and the *tat2Δ::HIS3* mutant FAB158 were used in this study.[16] To avoid confusion in focusing on tryptophan availability, YPH499 is solely designated the wild-type strain. Unless otherwise specified, cells were grown at 25 °C with shaking in synthetic dextrose (SD) medium containing 40 μg mL^{-1} L-tryptophan, or SD medium containing 4 μg mL^{-1} L-tryptophan (hereafter referred to as SD 4Trp). For a plate assay, cells were cultured on SD, SD 4Trp, and YPD at 25 °C for 3 days.

Error-Prone PCR on *TAT2*. Base substitutions were randomly introduced into *TAT2* by error-prone PCR[28] using primers 5′-GCACGACAGGTTTCCCGACTGG-3′ and 5′-ACCGCATCAGGCGCCATTCGCC-3′, and p3HA-TAT2c (3HA-tagged *TAT2* driven by its own promoter in YCplac33 [*URA3 CEN4*][29] as a template.[16] The reaction mixture contained 20 μM dATP, 1 mM dTTP, 1 mM dGTP, 1 mM dCTP, 5 mM $MgCl_2$, and varied concentrations of $MnCl_2$ (0.3−0.6 mM). The resulting DNA fragments and YEplac195 (*URA3* 2 μ)[29] digested with *Eco*RI/*Pst*I were introduced into YPH499 cells to obtain mutated *TAT2* plasmids using the gap-repair method. Approximately 500 transformant colonies were selected, and the cells were placed on fresh SD agar plates followed by incubation at 10, 15, and 25 °C. Cells defective in growth at 10 or 15 °C were assumed to be candidates that expressed dysfunctional Tat2 proteins. Plasmids were recovered from the candidates, and the entire *TAT2* open reading frame was sequenced to determine mutation sites.

Construction of Plasmids. Plasmids used in this study are listed in Table 1. PCR-based site-directed mutagenesis was performed to create amino acid substitutions in the Tat2 TMDs using a QuikChange II site-directed mutagenesis kit (Agilent Technologies Inc., Santa Clara, CA, USA) or PrimerSTAR mutagenesis basal kit (TaKaRa Bio Inc., Otsu, Shiga, Japan). p3HA-TAT2c was used as a template for PCR.[16] The appropriate base substitution was confirmed by sequencing the entire region of the *TAT2* ORF using the relevant sequence primers.

pSCU709 (13c-Myc-GFP-*CYC1* terminator, 2 μ, *URA3*), which was kindly provided by T. Ushimaru of Shizuoka University, was used to generate a plasmid containing *TAT2*-13c-Myc-GFP (hereafter referred to *TAT2*-GFP). pSCU709 was digested with *Sac*I and *Bam*HI to remove the *GAL1* promoter from the plasmid. The *TAT2* ORF and its own promoter region (800 bp upstream of the ORF) were amplified by PCR using the genomic DNA from strain YPH499 as a template and GGGAACAAAAGCTGGAGCTCCGCTTAAACCATCTGCAAGTCTCTTCCG and TTAATTAACCCGGGGGATCCACACCAGAAATGGAACTGTCTCACGTAC as primers (sequences complementary to the ends of the digested plasmid are underlined). The linearized plasmid and the PCR product were introduced into strain YPH499 to generate pSCU709-TAT2-GFP in cells based on homologous recombination. The plasmid was purified from the transformant cells using the conventional method, and the entire region of the *TAT2* ORF in the plasmid was sequenced. The plasmid was digested with *Sac*I and *Kpn*I, and the resulting *TAT2* fragment was introduced to YCplac33 to obtain the centromere-based *TAT2*-GFP plasmid, p3HA-TAT2-GFPc. PCR-based site-directed

Table 1. Plasmids Used in This Study

plasmid	description	source or reference
YCplac33	*URA3 CEN4*	29
YEplac195	*URA2* 2 μ	29
pSCU709	13c-Myc-GFP, *URA3* 2 μ	Provided by T. Ushimaru
p3HA-TAT2c	3HA-*TAT2* driven by *TAT2* promoter in YCplac33	16
p3HA-TAT2-I96Tc	3HA-*TAT2*-I96T driven by *TAT2* promoter in YCplac33	This study
p3HA-TAT2-G97Vc	3HA-*TAT2*-G97 V driven by *TAT2* promoter in YCplac33	This study
p3HA-TAT2-T98Ac	3HA-*TAT2*-T98A driven by *TAT2* promoter in YCplac33	This study
p3HA-TAT2-L100Sc	3HA-*TAT2*-L100S driven by *TAT2* promoter in YCplac33	This study
p3HA-TAT2-Y167Lc	3HA-*TAT2*-Y167L driven by *TAT2* promoter in YCplac33	This study
p3HA-TAT2-V168Ac	3HA-*TAT2*-V168A driven by *TAT2* promoter in YCplac33	This study
p3HA-TAT2-K228Rc	3HA-*TAT2*-K228R driven by *TAT2* promoter in YCplac33	This study
p3HA-TAT2-K228Qc	3HA-*TAT2*-K228Q driven by *TAT2* promoter in YCplac33	This study
p3HA-TAT2-I285Tc	3HA-*TAT2*-I285T driven by *TAT2* promoter in YCplac33	This study
p3HA-TAT2-E286Dc	3HA-*TAT2*-E286D driven by *TAT2* promoter in YCplac33	This study
p3HA-TAT2-E286Qc	3HA-*TAT2*-E286Q driven by *TAT2* promoter in YCplac33	This study
p3HA-TAT2-T288Ac	3HA-*TAT2*-T288A driven by *TAT2* promoter in YCplac33	This study
p3HA-TAT2-I311Lc	3HA-*TAT2*-I311L driven by *TAT2* promoter in YCplac33	This study
p3HA-TAT2-F313Lc	3HA-*TAT2*-F313L driven by *TAT2* promoter in YCplac33	This study
p3HA-TAT2-F314Lc	3HA-*TAT2*-F314L driven by *TAT2* promoter in YCplac33	This study
p3HA-TAT2-F315Lc	3HA-*TAT2*-F315L driven by *TAT2* promoter in YCplac33	This study
p3HA-TAT2-I317Lc	3HA-*TAT2*-I317L driven by *TAT2* promoter in YCplac33	This study
p3HA-TAT2-T320Lc	3HA-*TAT2*-T320L driven by *TAT2* promoter in YCplac33	This study
p3HA-TAT2-V322Lc	3HA-*TAT2*-V322L driven by *TAT2* promoter in YCplac33	This study
p3HA-TAT2-F324Lc	3HA-*TAT2*-F324L driven by *TAT2* promoter in YCplac33	This study
p3HA-TAT2-V326Lc	3HA-*TAT2*-V326L driven by *TAT2* promoter in YCplac33	This study
p3HA-TAT2-S370Gc	3HA-*TAT2*-S370G driven by *TAT2* promoter in YCplac33	This study
p3HA-TAT2-V371Ac	3HA-*TAT2*-V371A driven by *TAT2* promoter in YCplac33	This study
p3HA-TAT2-W446Lc	3HA-*TAT2*-W446L driven by *TAT2* promoter in YCplac33	This study
p3HA-TAT2-L447Sc	3HA-*TAT2*-L447S driven by *TAT2* promoter in YCplac33	This study
pTAT2-GFPc	*TAT2*-13c-Myc-GFP driven by *TAT2* promoter in YCplac33	This study
pTAT2-I96T-GFPc	*TAT2*-I96T-13c-Myc-GFP driven by *TAT2* promoter in YCplac33	This study
pTAT2-L100S-GFPc	*TAT2*-L100S-13c-Myc-GFP driven by *TAT2* promoter in YCplac33	This study
pTAT2-Y167L-GFPc	*TAT2*-Y167L-13c-Myc-GFP driven by *TAT2* promoter in YCplac33	This study
pTAT2-V168A-GFPc	*TAT2*-V168A-13c-Myc-GFP driven by *TAT2* promoter in YCplac33	This study
pTAT2-E286D-GFPc	*TAT2*-E286D-13c-Myc-GFP driven by *TAT2* promoter in YCplac33	This study
pTAT2-F315L-GFPc	*TAT2*-F315L-13c-Myc-GFP driven by *TAT2* promoter in YCplac33	This study
pTAT2-T320L-GFPc	*TAT2*-T320L-13c-Myc-GFP driven by *TAT2* promoter in YCplac33	This study
pTAT2-F324L-GFPc	*TAT2*-F324L-13c-Myc-GFP driven by *TAT2* promoter in YCplac33	This study
pTAT2-S370G-GFPc	*TAT2*-S370G-13c-Myc-GFP driven by *TAT2* promoter in YCplac33	This study

mutagenesis was performed to create amino acid substitutions in this plasmid as described above.

Western Blotting. Preparation of whole cell extracts was performed as described previously with a slight modification.[16] Briefly, 10^8 cells in exponential growth phase ($(1.0-1.5) \times 10^7$ cells mL^{-1}) were collected by centrifugation, washed serially with 10 mM NaN_3/10 mM NaF and lysis buffer A (50 mM Tris-HCl, 5 mM EDTA, 10 mM NaN_3, 1 mM PMSF, one tablet of Complete EDTA-free [Roche, Mannheim, Germany] for 50 mL, pH 7.5), and disrupted with glass beads at 4 °C. Unbroken cells and debris were removed by centrifugation at 900 × *g* for 5 min, and the cleared lysates were treated with 5% SDS and 5% 2-mercaptoethanol at 37 °C for 10 min to denature proteins. To obtain the P13 membrane fraction, the whole cell extracts were subjected to centrifugation at 13,000 × *g* for 10 min, and the resulting pellet were treated with 5% SDS and 5% 2-mercaptoethanol at 37 °C for 10 min. Monoclonal antibodies for HA (16B12, BabCO, Richmond, CA, USA), and Pma1 (EnCor Biotechnology Inc., Gainesville, FL, USA) were used. The signals were detected in an ImageQuant LAS4000 mini (GE Healthcare Life Sciences, Piscataway, NJ, USA).

Amino Acid Import Assay. The radiolabeled amino acids used were: L-[5-^{3}H] tryptophan (ART0244, 740 GBq mmol^{-1}, American Radiolabeled Chemicals, Inc., St. Louis, MO, USA), L-[ring-3,5-^{3}H] tyrosine (MT-887, 1.85 TBq mmol^{-1}, Moravek Biochemicals, Inc., Brea, CA, USA) and L-[2,4-ring-^{3}H]-phenylalanine (MT-1916, 610.5 GBq mmol^{-1}, Moravek Biochemicals). The amino acid uptake assay was performed as described previously with some modifications.[16] Cells were grown in SD medium at 25 °C at densities of up to 1.5×10^7 cells mL^{-1}. The cells were washed twice with SD 4Trp medium, and then cell culture was continued in SD 4Trp for an additional 5 h. The cells were collected by centrifugation, washed twice with SD medium lacking tryptophan (SD 0Trp), and resuspended in SD 0Trp at densities of around 3×10^7 cells mL^{-1}. The cell suspension was mixed with SD medium containing tryptophan, tyrosine, or phenylalanine at 39.2 μM, and 1/500 of the total volume of the radiolabeled materials. Consequently, the amino acid concentration in the import assay was 19.6 μM, corresponding to 4 μg mL^{-1} tryptophan, 3.55 μg mL^{-1} tyrosine, and 3.24 μg mL^{-1} phenylalanine. After 30 min incubation, the cells were trapped with a vacuum aspirator on GF/C glass filters stacked in pairs. The quantity of incorporated amino acids was measured using a liquid scintillation counter. In our experimental condition, 1 DPM for [5-^{3}H] tryptophan, L-[ring-3,5-^{3}H] tyrosine, and L-[2,4-ring-^{3}H]-phenylalanine can be converted to 6.4, 13.9, and 7.8 fmol of the amino acid incorporated into the cells, respectively. Data are expressed as mean values of amino acid incorporated (pmol 10^7 cells^{-1} min^{-1}) with standard deviations obtained from more than three independent experiments.

Fluorescence Microscopy. Cells expressing GFP-tagged Tat2 proteins were imaged on a fluorescence microscope model IX70 (Olympus, Co. Ltd., Tokyo, Japan).

dx.doi.org/10.1021/bi4004638 | *Biochemistry* 2013, 52, 4296−4307

Structural Modeling. The ESyPred3D Web Server 1.0 software (http://www.fundp.ac.be/sciences/biologie/urbm/bioinfo/esypred/), an automated homology modeling program with increased alignment performances based on the modeling package MODELER, was used.[30,31] The profile query for Tat2 yielded the *E. coli* arginine/agmatine antiporter AdiC (PDB entry: 3LRB and 3L1L) as a structural template.[25,27] An alignment was created for the template, and the Tat2 model was constructed using the PyMOL Molecular Graphics System, Version 1.5.0.4 Schrödinger, LLC (http://www.pymol.org/).[32]

RESULTS

Rationale for Mutation Design. We adopted two approaches to identify critical amino acid residues for Tat2-mediated tryptophan import. First, error-prone PCR was performed to create a *TAT2* multicopy plasmid library with random mutations. The wild-type *TAT2* in multicopy confers high-pressure and low-temperature growth on tryptophan-auxotrophic strains.[15] Screening of the library at 10−15 °C can yield dysfunctional *TAT2* plasmids that fail to confer low-temperature growth on a tryptophan-auxotrophic strain, and hence critical amino acid residues could be determined. Second, site-directed mutagenesis was performed based on the following criteria: (i) highly conserved residues among the yeast amino acid permeases; and (ii) Tat2 amino acid residues that corresponded to the sites shown by crystallographic and functional studies to be involved in substrate recognition and transport in the *E. coli* arginine/agmatine antiporter AdiC (see below).

Among ∼500 transformants obtained after error-prone PCR, 151 strains exhibited growth defects when cells were cultured at 10 and 15 °C for 10 days. These strains were subjected to Western blotting to select mutants that expressed levels of Tat2 proteins equivalent to the levels in wild-type cells. Then, we randomly selected 13 strains to sequence the entire *TAT2* coding region. At this stage, however, we failed to locate single amino acid residues that were responsible for Tat2 function because all 13 Tat2 variants contained more than two amino acid substitutions (data not shown). Nevertheless, we focused on some of the mutations to confine critical amino acid residues within the TMDs: I96T (TMD1), L100S (TMD1), V168A (TMD3), I285T (TMD6), T288A (TMD6), T320L (TMD7), F324L (TMD7), and L447S (TMD10). The location of TMDs in parentheses was predicted with HMMTOP transmembrane helices prediction software v 2 (http://www.enzim.hu/hmmtop/).[33] In addition to the eight mutations, we also mutated additional sites due to their potential significance. Despite the charged side chains, K228 (TMD5) and E286 (TMD6) appeared to be fully conserved among yeast amino acid permeases in the TMDs as shown by primary amino acid sequence alignments (Figure 1). The charges should be canceled by interacting with other polar amino acid residues within the lipid bilayer, or might be used to interact with external tryptophan molecules. In particular, E286 is conserved in *E. coli* AdiC (E208 of AdiC TMD6; see below). Thus, K228R, K228Q, E286D, and E286Q mutations were created.

TMD7 of Tat2 is relatively enriched in phenylalanine compared with other TMDs (Figure 1). Phenylalanine is enriched in π electrons, suggesting that $\pi-\pi$ interactions contribute to stabilizing TMD7, or that external tryptophan might first contact the phenylalanine side chains in Tat2 through $\pi-\pi$ interactions. Supporting this suggestion, the F324L mutation was obtained from the error-prone PCR experiments. Thus, F313L, F314L, and F315L substitutions were also introduced into TMD7. Based on a helical wheel projection algorithm (http://rzlab.ucr.edu/scripts/wheel/wheel.cgi), I317 appeared to locate on the same side of F324, whereas I311, V322, and V326 were located on the opposite side (data not shown). Then, I311L, I317L, V322L, and V326L substitutions were also introduced into Tat2. It should be noted that in the modeled Tat2 structures the amino acid sequence containing T320, V322, and F324 formed TMD7 when the AdiC substrate-binding occluded structure was the template. However, it formed a loop when the substrate-free outward-open structure was the template (see below). It was shown that S388 and V389 of Gap1 permease are used as amino acid binding sites and also mediate the activation of the PKA signaling pathway in the concept of a transceptor.[34] The corresponding sites in TMD8 were mutated in Tat2 to create S370G and V371A, respectively.

Structural models of Tat2 were constructed based on the sequence similarity afforded by ESyPred3D Web Server 1.0 using the crystal structures of *E. coli* AdiC (PDB: 3LRB and 3L1L) as templates, which exhibited the highest similarity scores among registered proteins in the PDB with 15% identity. Protein−protein BLAST exhibited scores of 21% identity and 39% similarity between Tat2 and AdiC. HHpred, another program for homology detection and structure prediction (http://toolkit.tuebingen.mpg.de/hhpred), also afforded AdiC (PDB: 3L1L) in the top score followed by *Methanocaldococcus jannaschii* Na^+-independent amino acid transporter ApcT (PDB: 3GIA), *E. coli* glutamate-GABA antiporter GadC (PDB: 4DJK), and *Microbacterium liquefaciens* nucleobase-cation-symport-1 family transporter Mhp1 (PDB: 2JLN). We found that the AdiC substrate-binding motifs, GSG (TMD1) and GVESA (TMD6), were only conserved in Tat2 but not in ApcT, GadC and Mhp1, and hence AdiC was used to build Tat2 structural models (see below). The sequence identity between Tat2 and AdiC is less than 30%, which is the generally accepted criterion for high-accuracy modeling allowing the TMDs to the native structure ones with <2 Å backbone root-mean-square deviations.[35−37] Thus, the modeled Tat2 structure leaves a certain level of ambiguity. Nevertheless, it provides useful information on the structure−function relationship in Tat2. The modeled Tat2 formed a pseudo-twofold symmetry perpendicular to the lipid membrane (Figure 2). We identified a trajectory along the perpendicular axis of Tat2 as the putative tryptophan pathway (Figure 2). The central cavity lies within the middle of Tat2 and was assumed to be the tryptophan-binding pocket that corresponded to the arginine-binding pocket of AdiC.[27] The trajectory as viewed from the top seemed to be closed in the substrate binding-occluded Tat2 model (Figure 2). It was shown that TMD1, −3, −6, −8, and −10 were located in the interior of the overall folding of AdiC. The GSG motif (residues 25−27) of AdiC is located within the helix break of TMD1 and plays a role in recognition of the carboxyl group of the substrate.[25,27] The corresponding site of Tat2 TMD1 is GTG (residues 97−99), which is located adjacent to the residues obtained by error-prone PCR (I96T and L100S). Thus, two residues were mutated in Tat2 to yield G97 V and T98A in TMD1. The GVESA motif (residues 206−210) of AdiC is located within the helix break of TMD6 and plays a role in recognition of the amino group of the substrate.[25,27] The corresponding site of Tat2 TMD6 is GIEMT (residues 284−288), in which amino acid residues that had been obtained by error-prone PCR were located (I285T and T288A). The central cavity of AdiC consists of N22 and S26 from TMD1, Y93 from TMD3, E208 from TMD6, and Y365 from TMD10, which correspond

dx.doi.org/10.1021/bi4004638 | *Biochemistry* 2013, 52, 4296−4307

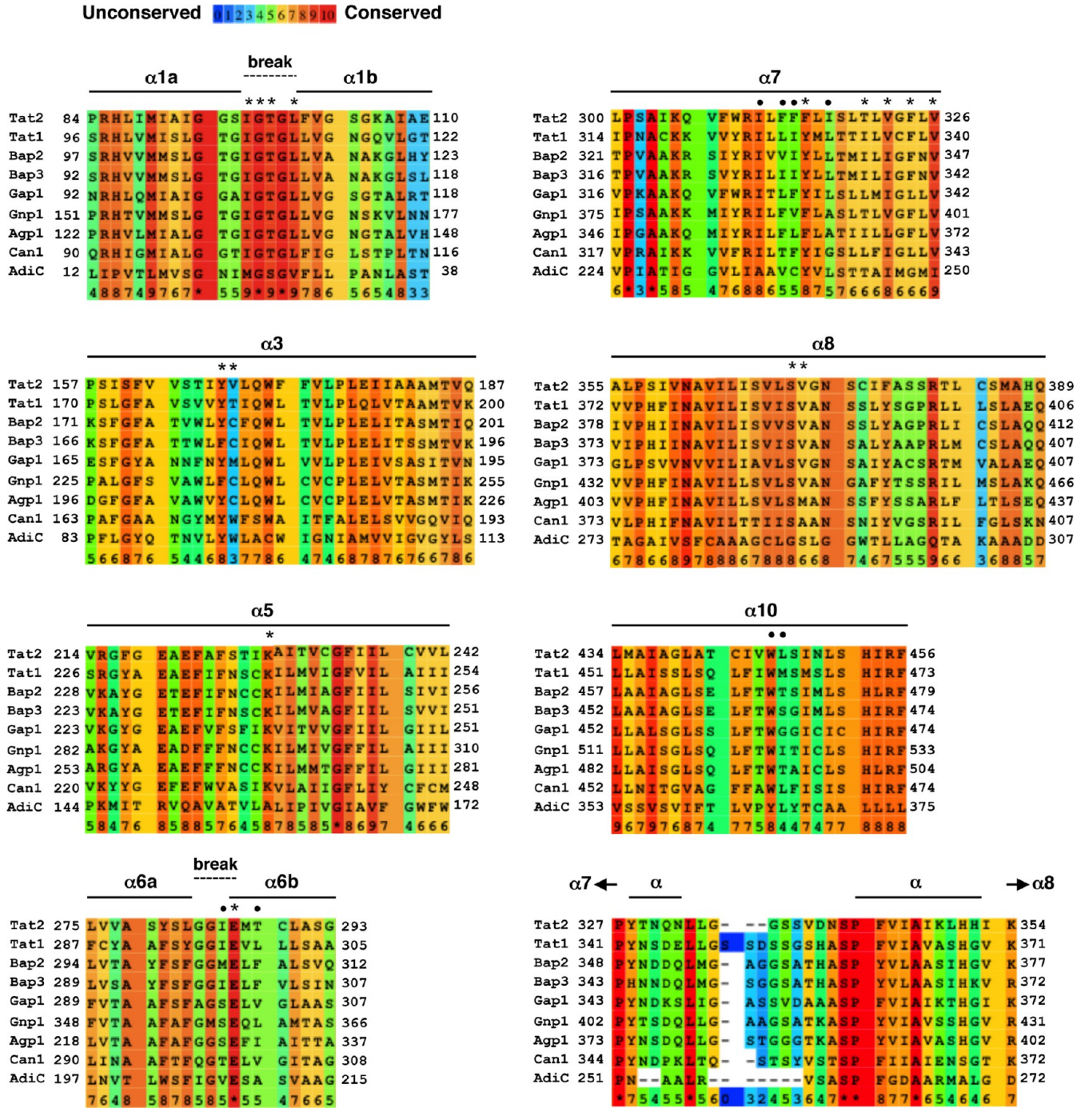

Figure 1. Multiple sequence alignments of TMD α-helix 1, −3, −5, −8, and −10 of Tat2, some amino acid permeases of *S. cerevisiae* and *E. coli* AdiC. Residues mutated in this study are marked on the top. The alignments were constructed using the PRALINE multiple-sequence alignment program.[54] TMD α-helices were assigned based on the crystallographic structures of AdiC (PDB: 3L1L).[27] TMDα1 and TMDα6 are divided by an α-helix break to give TMDα1a/TMDα1b and TMDα6a/TMDα6b, respectively, according to the AdiC structure (PDB: 3L1L).[27] Amino acid residues essential for Tat2-mediated tryptophan import are indicated by asterisks (*), and residues prone to mutation are indicated by dots (•). α denotes α-helix. The numbers in the bottom rows indicate consistency scores derived in PRALINE.

to G94, T98, Y167, E286, and W446 in Tat2, respectively. Therefore, Y167L and W446L mutations were introduced into Tat2 in addition to T98A and E286D. In total, 23 amino acid residues were replaced individually in Tat2 (Figure 1 and Table 2).

Functional Analysis of Tat2 Mutant Proteins. Initially, we evaluated Tat2 mutations based on colony formation at 10 or 15 °C in the wild-type strain bearing the mutant *TAT2* multicopy plasmids. However, this assay requires a long time (~10 days) to determine colony growth, which was sometimes unclear. Therefore, we finally examined whether the mutant *TAT2* in centromere-based plasmids complemented growth defects of the *tat2*Δ mutant FAB158 at 25 °C. In normal SD medium containing 40 μg mL^{-1} tryptophan, the growth of the *tat2*Δ mutant can be supported by Tat1 function but not in SD medium supplemented with high concentrations of phenylalanine and tyrosine (100 μg mL^{-1} each) or YPD medium.

dx.doi.org/10.1021/bi4004638 | *Biochemistry* 2013, 52, 4296−4307

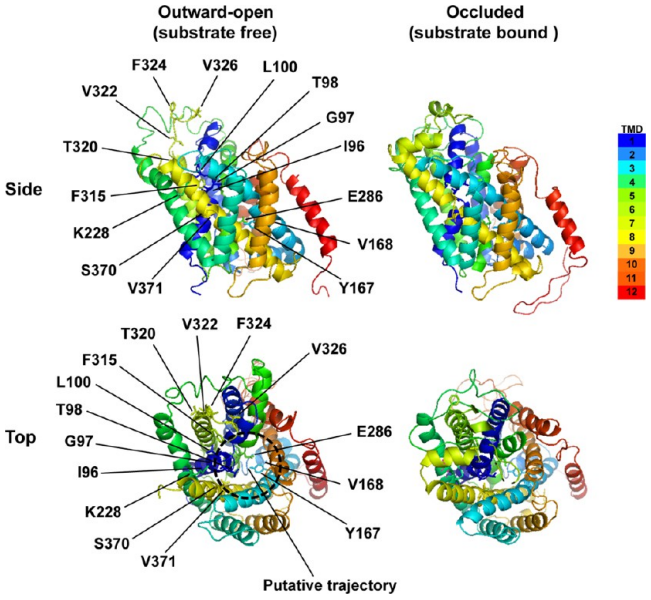

Figure 2. Structural models of Tat2. Overall structures of Tat2 based on the AdiC outward-open (left, PDB: 3LRB as a template) and occluded (right, PDB: 3L1L as a template) crystal structures. Essential amino acid residues for tryptophan import are shown. The putative trajectory is circled.

Table 2. Mutated Amino Acid Residues in Tat2 and Corresponding AdiC Residues

Tat2 mutation	TMD[a]	Tat2 function[b]	corresponding AdiC residue
I96T	1	−	M24
G97 V	1	−	G25
T98A	1	−	S26
L100S	1	−	V28
Y167L	3	−	Y93
V168A	3	−	W94
K228R	5	−	A158
K228Q	5	−	A158
I285T	6	+	V207
E286D	6	−	E208
E286Q	6	−	E208
T288A	6	+	A210
I311L	7	+	A235
F313L	7	+	V237
F314L	7	±	C238
F315L	7	−	Y239
I317L	7	±	L241
T320L	7	−	T244
V322L	7	−	I246
F324L	7	−	G248
V326L	7	−	I250
S370G	8	−	G288
V371A	8	−	S289
W446L	10	±	Y365
L447S	10	±	L366

[a]TMDs were assigned based on the crystallographic structure of AdiC (PDB: 3L1L). [b]Tat2 funciton was elvaluated by the complementation test for growth on SD 4Trp and YPD in the *tat2*Δ strain expressing the mutant Tat2. −, no growth; ±, poor growth; +, growth.

This is because Tat1-mediated tryptophan uptake is competitively inhibited by phenylalanine and tyrosine.[16] We found that the *tat2*Δ mutant was also defective in growth on low-tryptophan (SD 4Trp) medium due to inefficient tryptophan uptake by Tat1 (Figure 3). Therefore, any mutations affecting Tat2

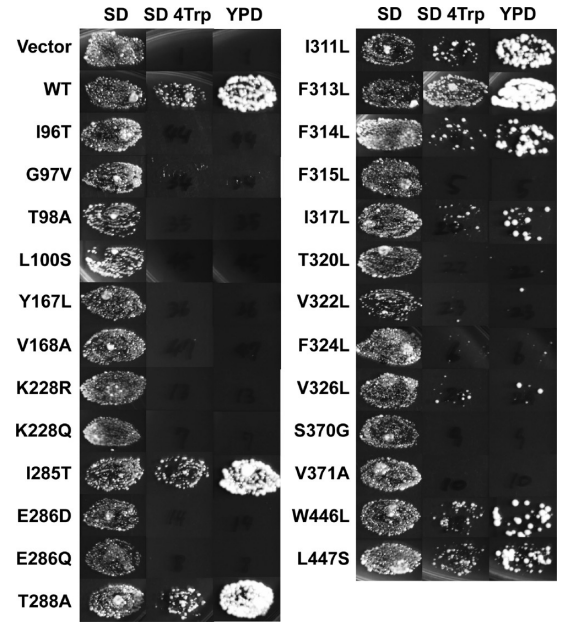

Figure 3. Effects of Tat2 mutations on cell growth. Tat2 mutant proteins were expressed in *tat2*Δ cells. The cells were incubated on SD, SD 4Trp, and YPD plates at 25 °C for 3 days.

function could be revealed by growth tests on SD 4Trp and YPD at 25 °C. It should be noted that the growth test has to be performed at 25 °C but not at higher temperatures (e.g., 30 °C) because the *tat2*Δ mutant exhibits slow growth on YPD at 30 °C (data not shown). Figure 3 shows that Tat2 mutants carrying the 23 amino acid substitutions exhibited varied ability to grow on SD 4Trp and YPD. They were classified into three groups: (i) the F315L, F324L, S370G, V371A, K228R, E286D, T320L, V322L, V326L, G97V, T98A, Y167L, I96T, L100S, and V168A mutations conferred severe growth defects; (ii) the F314L, I317L, W446L, and L447S mutations conferred moderate defects; and (iii) the F313L, I311L, I285T, and T288A mutations had no measurable effect on growth. Mutant strains defective in growth in SD 4Trp were always also defective in growth in YPD medium.

Expression and Localization of Tat2 Mutant Proteins. For subsequent analyses, we selected the I96T, L100S, Y167L, V168A, E286D, F315L, T320L, F324L, and S370G mutations based on the criteria of severity of defective growth and potential importance according to the studies on AdiC. For the results of tryptophan import assays to be valid, the plasma membrane localization of Tat2 must be confirmed. Under normal or high tryptophan concentrations (20−200 μg mL^{-1}), Tat2 is not efficiently delivered to the plasma membrane, but preferentially targeted to the vacuole for degradation.[38] Upon the shift to low-tryptophan medium (e.g., 4 μg mL^{-1}), Tat2 is efficiently delivered to the plasma membrane.[38] Thus, we cultured the cells in SD 4Trp medium after overnight culture in SD medium. Upon shifting the cells to SD 4Trp, the OD_{600} values increased by 1.7- to 2-fold in 5 h regardless of the mutations, suggesting that the mutant cells continued proliferation even at the beginning of the low-tryptophan shift. However, we noted that extended culture time in SD 4Trp (>7 h) reduced Tat2^{E286D}-GFP and Tat2^{F315L}-GFP from the plasma membrane for vacuolar degradation (data not shown).

dx.doi.org/10.1021/bi4004638 | *Biochemistry* 2013, 52, 4296−4307

Therefore, 5 h after the low-tryptophan shift is the most appropriate time to evaluate Tat2 function.

We confirmed Tat2 expression in the P13 membranes after 5-h culture of *tat2*Δ cells bearing HA-tagged *TAT2* plasmids in SD 4Trp medium. Whereas the Y167L, V168A, T320L, F324L, and S370G mutations had no measurable effect on Tat2 quantity, the I96T, L100S, E286D, and F315L mutations led to a slight decrease in the Tat2 level (Figure 4). Although Tat2

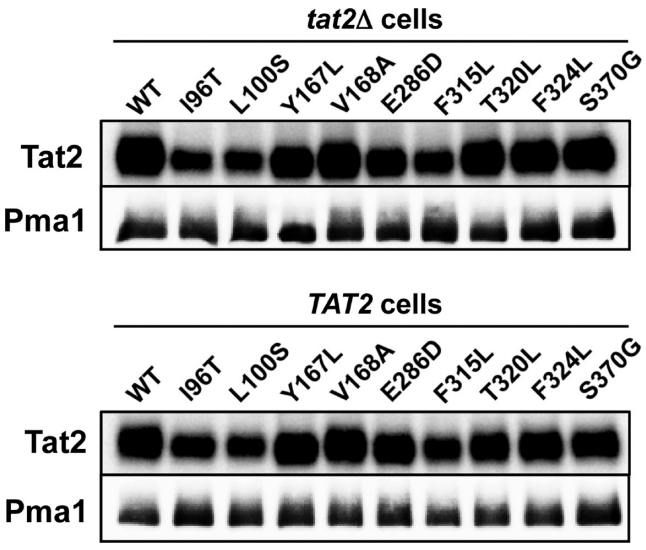

Figure 4. Expression of Tat2 mutant proteins. Tat2 mutant proteins were expressed in *tat2*Δ cells (A) or in the wild-type cells (B). Exponentially growing cells in SD medium were shifted to SD 4Trp medium, followed by additional 5 h incubation. The P13 membranes were collected by centrifugation at 13,000 × *g* for 10 min. The membranes were subjected to Western blot analysis to detect 3HA-Tat2 and Pma1 using specific monoclonal antibodies.

was expressed in the wild-type (*TAT2*) cells, the I96T, L100S, E286D, and F315L mutations also led to slightly reduced Tat2 expression as observed in *tat2*Δ cells (Figure 4), suggesting that the three mutations affect the trafficking or stability of Tat2. Nevertheless, we assumed that the expression levels of these mutant Tat2 proteins were sufficient for amino acid import analysis. Because of the low expression level, GFP-tagged wild-type Tat2 slightly localized to the plasma membrane. We confirmed that Tat2-GFP also localized to the plasma membrane regardless of the mutations (Figure 5), which in turn justifies the subsequent amino acid import assay.

Uptake of Tryptophan, Tyrosine, and Phenylalanine by Tat2 Mutants. It was shown that tryptophan is mainly imported by Tat2 and to a lesser extent by Tat1, and tyrosine is imported solely by Tat1.[11] Phenylalanine import has not been examined previously. In that previous study, the uptake was measured in the absence of non-radiolabeled amino acids in sodium citrate buffer, i.e., radiolabeled tryptophan and tyrosine were the sole substrates for the import assay.[10,11] Thus, the concentrations of tryptophan and tyrosine were extremely low when measured. In our present study, we ensured consistent amino acid uptake with the ability to grow in SD 4Trp by performing the measurements at a concentration of 19.6 μM of each amino acid (4 μg mL^{-1} tryptophan; 3.55 μg mL^{-1} tyrosine; 3.24 μg mL^{-1} phenylalanine) in the presence of trance amounts of radiolabeled materials (<60 nM each) at 1000-fold dilution. The import rates measured in *tat2*Δ cells

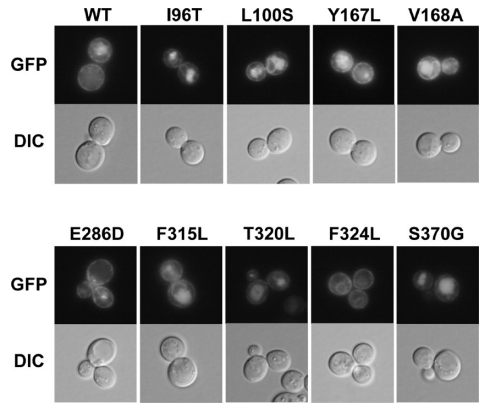

Figure 5. Localization of Tat2 mutant proteins. GFP-tagged Tat2 mutant proteins were expressed in *tat2*Δ cells. Exponentially growing cells in SD 4Trp medium were imaged in a fluorescence microscope.

corresponded to those mediated by Tat1. We found that Tat1 imported tryptophan, tyrosine, and phenylalanine at a rate of 0.93, 3.3, and 2.4 pmol 10^7 cells^{-1} min^{-1}, respectively (Figure 6A, vector). This level of tryptophan import could be insufficient to support cell growth on SD 4Trp medium (Figure 3). Otherwise, Tat1 might be down-regulated when cells are cultured on SD 4Trp for 2−3 days. The efficient tyrosine import by Tat1 is in agreement with previous results.[11] Phenylalanine import by Tat1 was intermediate between that of tryptophan and tyrosine. The rates of net Tat2-mediated import could be estimated by subtracting the rate for vector alone from that of the wild-type Tat2, which were 1.4 (tryptophan), 1.3 (tyrosine), and 1.6 (phenylalanine) pmol 10^7 cells^{-1} min^{-1} (Figure 6B, WT). Accordingly, Tat2 appeared to import the three aromatic amino acids at almost equivalent rates when other competitive substrates were absent. In contrast, Tat1 preferred tyrosine, phenylalanine, and tryptophan in this order for import. According to our previous quantification by Western blotting, Tat1 is 9-fold more abundant than Tat2.[16] Thus, the specific tryptophan import activity of Tat2 is much greater than that of Tat1. Although an experiment should be performed using a *tat1*Δ*tat2*Δ double-deletion mutant, we failed to disrupt both genes against the YPH499 tryptophan-auxotrophic background, probably due to lethality. We found that the nine Tat2 mutations significantly abolished the import of the three amino acids, including a moderate effect of the F320L mutation. In some cases, amino acid uptake of mutants was less than that of the *tat2*Δ cells for unknown reasons (Figure 6A). Consequently, the net Tat2-mediated uptake showed negative values in Y167L and F315L (tyrosine), and F315L and S370G (phenylalanine) (Figure 6B). Interestingly, the V168A mutation had a more pronounced decrease in tryptophan import than in tyrosine or phenylalanine import (Figure 6B). Although this effect was not marked, V168 and other amino acid residues in its vicinity would offer a clue to understanding the role of tryptophan recognition and translocation through Tat2.

Structural and Functional Insights into Tat2-Mediated Tryptophan Import. The Tat2 structural model was based on the AdiC substrate-free outward-open structure (PDB: 3LRB) and the arginine-bound occluded structure (PDB: 3L1L) as templates (Figure 2).[25,27] Upon arginine binding, AdiC undergoes major conformational changes in TMD2, TMD6, and TMD10, of which TMD6 exhibits the most pronounced structural shift. The entire TMD6a (the *N*-terminal half of TMD6) of AdiC pivots around the unwound region by approximately 40°, resulting

dx.doi.org/10.1021/bi4004638 | *Biochemistry* 2013, 52, 4296−4307

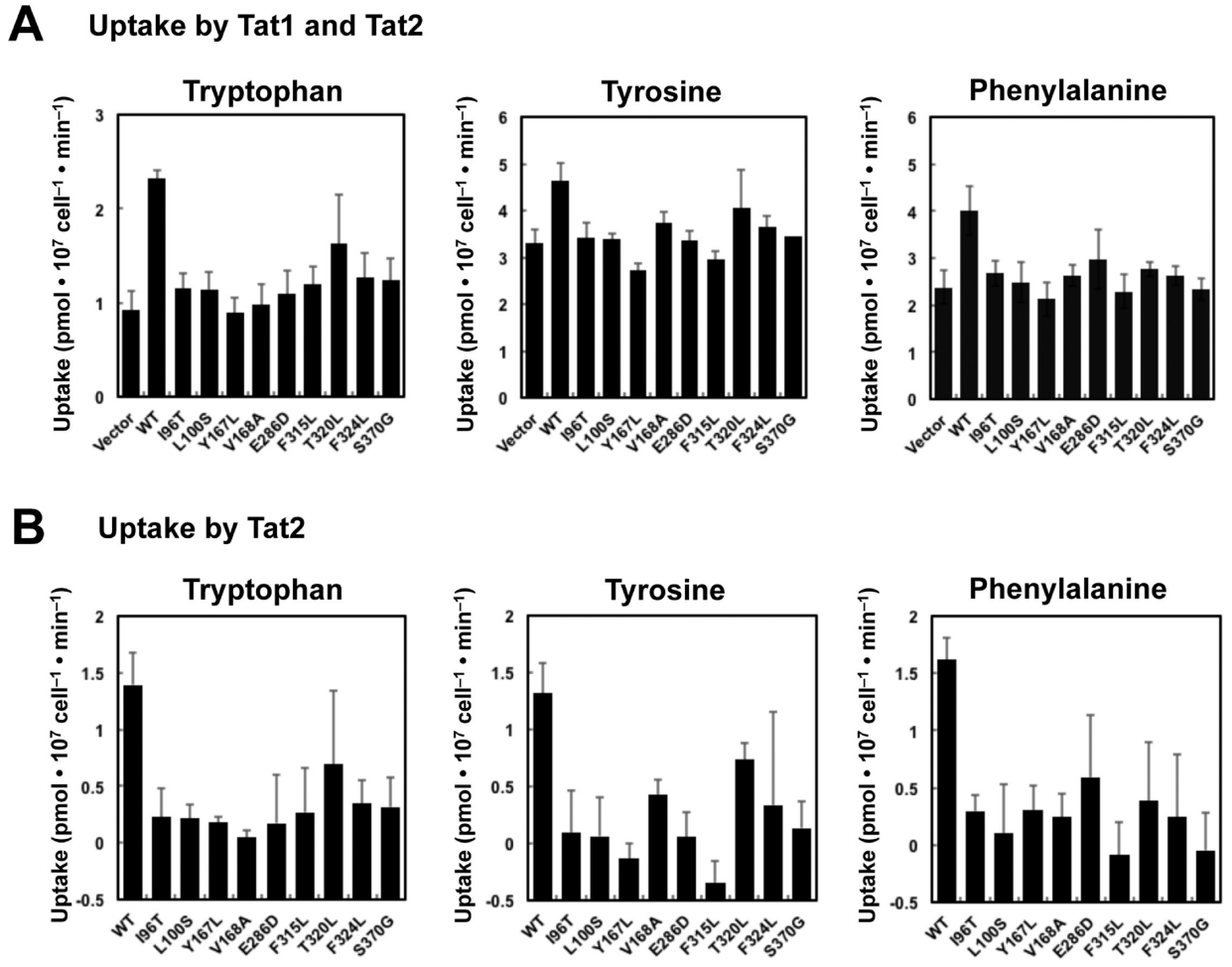

Figure 6. Effects of Tat2 mutations on tryptophan, tyrosine, and phenylalanine import. Tat2 mutant proteins were expressed in *tat2*Δ cells. (A) Exponentially growing cells in SD medium were shifted to SD 4Trp medium, followed by additional 5 h incubation. Uptake of the amino acids was measured as described in Materials and Methods. (B) The amino acid import rates in *tat2*Δ cells were subtracted from those in the wild-type or Tat2 mutant cells. Data are expressed as mean values of amino acid incorporated (pmol 10^7 cells^{-1} min^{-1}) with standard deviations obtained from more than three independent experiments.

in the occluded state.[27] Corresponding structural alterations in TMD2, TMD6, and TMD10 were recognized by comparing the two modeled Tat2 structures (Figure 7A). Along with the swinging movement of AdiC TMD6a, the aromatic side-chain of W202 is translocated to interact with the aliphatic portion of arginine and block its exit route back to the periplasm.[27]

The positively charged α-amino group of arginine donates three hydrogen bonds to the carbonyl oxygen atoms of I23, W201, and I205 in AdiC. The α-carboxylate group of arginine accepts two hydrogen bonds from the side chain of S26 and the amide nitrogen of G27, and both residues are located on the helix-breaking GSG motif of TMD1. The amino acid residues of Tat2 corresponding to I23, W201, I205, S26, and G27 of AdiC are S95 (TMD1), G283 (TMD6), Y280 (TMD6), T98 (TMD1), and G99 (TMD1). Notably, G283, Y280, T98, and G99 are highly conserved in the yeast amino acid permeases, all of which are located within or adjacent to the helix-breaking regions of TMD1 and TMD6 (Figure 1). Mutations around the helix-breaking regions such as I96T, G97V, T98A, and L100S (TMD1) and E286D (TMD6) compromised Tat2-mediated tryptophan import (Figure 3). The G99A mutation also abolished Tat2 function (data not shown). Therefore, the α-amino and α-carboxylate group of tryptophan possibly binds to the aforementioned amino acid residues in the helix-breaking regions of Tat2, and this is also likely in other yeast amino acid permeases. On the other hand, the guanidinium group of arginine interacts with A96, C97, N101, W293, and S357 in AdiC,[27] which correspond to Q170, a gap, V174, C375, and A438 in Tat2 (Figure 1). These amino acid residues are variable among the yeast amino acid permeases and thereby possibly have a role in determining substrate specificity.

In the layer distal to the periplasm in AdiC, Y93 (TMD3), E208 (TMD6), and Y365 (TMD10) play a central role in arginine transport as the distal gate.[27] The hydrogen bond network surrounding E208 is thought to lock TMD3, TMD6, and TMD10 in a closed conformation, blocking substrate transport. Arginine binding between W202 and W293 leads to the translocation of W293 and a conformational shift of TMD8, allowing arginine to sink and come into contact with the distal gate. Such contact is thought to disrupt interactions between E208 and Y93/Y365, causing additional changes in TMD3 and TMD10 to form an inward-open conformation of AdiC.[27] The amino acid residues of Tat2 corresponding to Y93, E208, and Y365 of AdiC are Y167, E286, and W446, of which E286 is fully and Y167 and W446 are highly conserved among the yeast amino acid permeases (Figure 1). The Y167L and E286D mutations abolished Tat2 function, while the W446L mutation caused a moderate defect (Figure 3), suggesting the existence

dx.doi.org/10.1021/bi4004638 | *Biochemistry* 2013, 52, 4296−4307

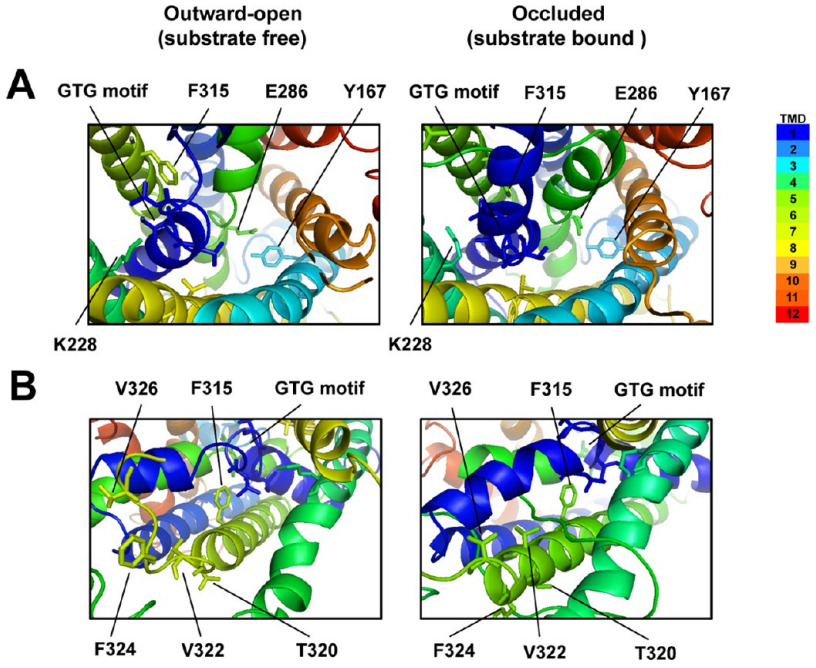

Figure 7. Structural models of Tat2. (A) Close-up view of the putative tryptophan-binding cavity. Interactions of E286-Y167 and F315-GTG motif-K228 are assumed. (B) Close-up view around TMD7. Whereas F320, V322, F324, and V326 are located in a loop in the outward-open structure (left), the residues are located on the TMD7 α-helix (right). The structural models were created with PyMOL software version 1.5.

of a gate for tryptophan consisting of Y167 and E286 and possibly another amino acid residue(s) (Figure 6B). In our unpublished observations, amino acid residues in Tat1 and leucine permeases Bap2/Bap3 corresponding to E286 of Tat2 are also essential for their substrate import activity, strongly supporting their crucial role. We also propose the working hypothesis that E286 may have a role in proton influx associated with tryptophan import (see Discussion).

Critical amino acid residues were also identified in TMD5, TMD7, and TMD8, of which the corresponding sites have not been focused in the crystallographic studies of AdiC. In the Tat2 model structure, K228 (TMD5) faces I96 and G97 in TMD1 (Figure 7B). Thus, the K228R mutation might indirectly abrogate the interaction of T98/G99 with the α-carboxylate group of tryptophan. In this vicinity, F315 (TMD7) might donate π electrons to the aliphatic side chain of L100 for structural stabilization (π-aliphatic chain interactions). Similarly, F324 (TMD7) might donate π electrons to H250 (TMD5) for stabilization (π-cation interactions). Whereas the critical amino acid residues T320, V322, F324, and V326 are located in TMD7 in the occluded Tat2 model, these residues are located in the extracellular loop between TMD7 and TMD8 in the outward-open model (Figure 7B). The following sequence containing amino acid residues from T329 to K354 did not form any structure in the outward-open Tat2 model, while it formed two short α-helices in the occluded Tat2 model, reflecting the AdiC structural templates (PDB: 3LRB and 3L1L, respectively). According to calculations using Gaussian network modeling, arginine binding to AdiC stabilizes the extracellular loop between TMD7 and TMD8, suggesting that such a structural rearrangement may cause a conformational shift of TMD8 allowing the opening of the middle gate of AdiC.[39] Therefore, T320L, V322L, F324L, and V326L mutations in Tat2 might abrogate the structural transition of the extracellular loop upon tryptophan binding, resulting in compromised tryptophan import. S370 and V371 of Tat2 correspond to S388 and V389 of Gap, respectively. S388 (TMD8) and V389 (TMD8) are exposed to the putative amino acid import pathway of Gap1 and are required for triggering the PKA pathway.[34] S370 and V371 are highly conserved among the yeast amino acid permeases (Figure 1). Whether Tat2 has the dual function of both transporter and receptor remains to be elucidated.

DISCUSSION

In this study, we identified critical amino acid residues for Tat2-mediated tryptophan import using random mutagenesis and rational site-directed mutagenesis based on the crystal structure of the *E. coli* arginine/agmatine antiporter AdiC. The growth assay of Tat2 mutants on SD 4Trp and YPD plates is a simple, effective way to discover dysfunctional Tat2 mutations when combined with the tryptophan-auxotrophic *tat2*Δ genetic background. Of the 23 amino acid residues tested, 15 were revealed to be essential while 8 were not. The GTG (TMD1) and GIEMT (TMD6) motifs, which correspond to the GSG and GVESA motifs of AdiC, respectively, are highly conserved among yeast amino acid permeases. Mutational analysis in combination with structural modeling led us to propose the working hypothesis that amino acid-binding architecture is likely to be analogous in AdiC and Tat2, and probably in other yeast amino acid permeases, with respect to interactions with the α-amino and α-carboxyl groups. However, the mechanisms by which substrate specificity and affinity are determined remain to be elucidated in the yeast amino acid permeases. At the substrate concentration in our assay (19.6 μM each), Tat2 imported tryptophan at a rate equivalent to the import of tyrosine and phenylalanine, whereas Tat1 imported tyrosine more efficiently than tryptophan and phenylalanine. In this sense, the tryptophan specificity of Tat1 and Tat2 was characterized in a relative manner. We showed that the V168A mutation abrogated tryptophan import compared with tyrosine import. Interestingly, V168 is the least conserved residue in TMD3 of the yeast amino acid permeases (Figure 1). In this way, amino acid residues in which mutations exclusively

dx.doi.org/10.1021/bi4004638 | *Biochemistry* 2013, 52, 4296−4307

abrogate tryptophan import, but not tyrosine and phenylalanine import, should exist in Tat2 to identify substrate-recognition mechanisms.

In the modeled Tat2 structure, E286 is located in the vicinity of Y167 at a reasonable distance to form a hydrogen bond (~0.3 nm). These residues are hypothesized to lock inward translocation of tryptophan molecules. The reduction of only a single CH_2-group (E286D) resulted in compromised tryptophan import, suggesting that subtle interaction is critical. Our analyses led to two working hypotheses that E286 also mediates proton influx coupled to tryptophan import. First, Pma1 extrudes protons to a great extent, possibly allowing the juxtamembrane extracellular region to become more acidic than the growth medium (pH 5–6). If the juxtamembrane pH is much less than 4, the majority of the E286 carboxyl chain of Tat2 is protonated (pK_a of glutamate ~4.07) in the outward-open structure. Upon tryptophan binding and the concomitant conformational change to form the inward-open structure, the E286 carboxyl chain releases protons in the cytoplasm at neutral pH. Second, the pK_a of E286 in Tat2 does not necessarily approximate that of glutamate in water. For example, pK_a of acetic acid is 4.76 in water but is 6.76 in 80% ethanol, for which the dielectric constant (D) is much lower than that of water (D_{water} ~80; $D_{80\%\ ethanol}$ ~34).[40] If the tryptophan binding and closure of Tat2 in the outward-facing occluded state releases water molecules to the solvent, the pK_a of E286 is likely to increase, so that it gets loaded with a proton. Then the pK_a decreases upon tryptophan release in the inward-facing open conformation, so that it releases the proton. These two models explain the kinetics of H^+-coupled amino acid symporters in yeast and possibly other H^+/solute symporters in a variety of organisms. It should be noted that the glutamate at the E286 position is highly conserved in TMD6 in a broad range of solute transporters including the *E. coli* phenylalanine permease PheP, aromatic amino acid permease AroP, or γ-aminobutyric permease GabP as well as AdiC and yeast amino acid permeases. Our hypotheses are in good agreement with the recent finding on Pho84 phosphate/H^+ transceptor in which D358 in TMD7 is the putative proton-binding site.[41] Alleles mutated in D358 abolish phosphate transport activity by Pho84 but are still capable of activating the PKA pathway, suggesting that transport and signaling functions can be separated.

Measurements of the rate constant of tryptophan import as a function of hydrostatic pressure revealed that Tat2 is associated with a dramatic increase in $\Delta V‡$ (50.8 mL mol^{-1}).[16] In contrast, leucine import is accompanied by a relatively small $\Delta V‡$ (24 mL mol^{-1}).[42] According to the proposed model,[43−45] $\Delta V‡$ is accounted for by summing three volume changes, $\Delta V‡_{(interaction)}$ + $\Delta V‡_{(conformation)}$ + $\Delta V‡_{(hydration)}$, where $\Delta V‡_{(interaction)}$ is the volume change accompanied by the formation and deformation of various interactions between the substrate and amino acid residues, $\Delta V‡_{(conformation)}$ is the volume change of the protein conformation, and $\Delta V‡_{(hydration)}$ is the volume change accompanied by modification of the hydration density resulting from the movement of specific amino acid residues into or away from contact with water. Although it is difficult to discriminate the three volume changes from one another, they could be positive values, assuming that (i) internal interactions break in order to bind tryptophan ($\Delta V‡_{(interaction)} > 0$), (ii) tryptophan binding and closure of the protein releases water of solvation of Tat2 and tryptophan to the bulk solvent ($\Delta V‡_{(hydration)} > 0$), and (iii) expansion of the Tat2 protein to import the bulky size of tryptophan ($\Delta V‡_{(interaction)} > 0$). In the case of pressure-induced unfolding of staphylococcal nuclease, internal cavities are the primary determinants, rather than increased amounts of surface area exposed to the solvent.[46] Filling a cavity dramatically increases the stability of a transcription factor c-Myb R2 subdomain under high pressure.[47] Essential amino acid residues T320, V322, and F324 are located in a loop in the outward-open substrate-free modeled Tat2, but the residues are located in TMD7 in the substrate-bound occluded modeled Tat2, reflecting the two AdiC structural templates (PDB: 3LRB and 3L1L, respectively). This offers an intriguing account for the large $\Delta V‡$ of Tat2-mediated tryptophan import by the loop-to-helix shift upon tryptophan binding, although the transition-state ensemble cannot be determined structurally and does not correspond to the tryptophan-bound occluded state of Tat2. It is worthwhile elucidating whether any Tat2 mutations affect the $\Delta V‡$ for tryptophan import.

LeuT is a bacterial homologue of the neurotransmitter:sodium symporter (NSS) family and is the only NSS member to have been structurally characterized by X-ray crystallography.[48,49] LeuT functions as a sodium-dependent aliphatic and aromatic amino acid symporter and imports a broad range of amino acids. However, tryptophan cannot be imported and is a competitive inhibitor. Unlike other LeuT-substrate-bound occluded structures, the LeuT-tryptophan complex adopts an open-to-out conformation because of the bulky size of tryptophan relative to the binding site. The I359Q mutation in LeuT converts the activity of tryptophan from an inhibitor to a transportable substrate, allowing the formation of the occluded state.[50] The I359Q mutation not only leads to a single change in the residue 359 side chain but also introduces both steric and electrostatic changes in the binding site which influence the conformation of the indole ring of the bound tryptophan to rotate downward toward the intracellular side of LeuT.[50] Therefore, the Tat2 mutations shown in this study could also influence both the tryptophan import pathway and binding kinetics, leading to compromised tryptophan import. In a study aiming at the determination of intracellular regions of Gap1 for appropriate trafficking in the cell, alanine-scanning mutagenesis was performed to replace consecutive three to four amino acid residues to alanines. Among the 64 Gap1 mutant alleles, six abrogated the L-citrulline import by Gap1 without affecting the plasma membrane localization.[51] Among the six sequences, five were located in juxtamembrane regions to TMD1, TMD5, or TMD6. In this sense, the intracellular domains of the yeast amino acid permeases might also influence the dynamic conformational changes in TMDs associated with substrate import. Topological modeling of the yeast monocarboxylate/H^+ symporter Jen1 based on the crystal structure of GlpT, an antiporter of glucerol-3-phosphate/inorganic phosphate in *E. coli*,[52] revealed a substrate translocation trajectory within the Jen1 molecule.[53] The structural modeling of the Pho84 phosphate/H^+ transceptor on the basis of the GlpT crystal structure revealed that D358 in TMD7 and K492 in TMD10 were critical amino acid residues for the transport function being part of the putative substrate-binding pocket of Pho84.[41]

Currently, detailed biochemical and biophysical analyses of Tat2 function are limited in terms of experiments performed in the whole-cell system. For example, the plasma membrane localization and abundance of Tat2 proteins depend on multiple factors such as the external tryptophan concentration, activity of Rsp5 ubiquitin ligase, and mutations in the Tat2 protein. Therefore, the purification and reconstitution of Tat2

dx.doi.org/10.1021/bi4004638 | *Biochemistry* 2013, 52, 4296−4307

in membranes are prerequisites for the evaluation of Tat2 mutations based on accurate determination of the K_m and k_{cat} values for tryptophan import. Nevertheless, our present study provides important clues to understanding substrate import mechanisms, not only in Tat2, but also in the yeast amino acid permeases.

AUTHOR INFORMATION

Corresponding Author

*Phone: +81-42-759-6233. Fax: +81-42-759-6511. E-mail: abef@chem.aoyama.ac.jp.

Notes

The authors declare no competing financial interest.

ACKNOWLEDGMENTS

We thank Mao Kaneko and Takahiro Mochizuki for technical assistance, Takashi Ushimaru for providing a GFP plasmid, Keietsu Abe and Kei Nakatani for critical reading of the manuscript, and Yoichi Noda, Nobuhisa Watanabe, Satoshi Uemura, and Makiko Suwa for valuable discussions. This work was supported by grants from the Japan Society for the Promotion of Science (No. 22658031 and No. 24580122 to F. Abe).

REFERENCES

(1) Rose, D. P. (1972) Aspects of tryptophan metabolism in health and disease: a review. *J. Clin. Pathol. 25*, 17−25.

(2) Stone, T. W., Mackay, G. M., Forrest, C. M., Clark, C. J., and Darlington, L. G. (2003) Tryptophan metabolites and brain disorders. *Clin. Chem. Lab. Med. 41*, 852−859.

(3) Ruddick, J. P., Evans, A. K., Nutt, D. J., Lightman, S. L., Rook, G. A., and Lowry, C. A. (2006) Tryptophan metabolism in the central nervous system: medical implications. *Expert Rev. Mol. Med. 8*, 1−27.

(4) Stone, T. W., Stoy, N., and Darlington, L. G. (2013) An expanding range of targets for kynurenine metabolites of tryptophan. *Trends Pharmacol. Sci. 34*, 136−143.

(5) Kim, D. K., Kanai, Y., Chairoungdua, A., Matsuo, H., Cha, S. H., and Endou, H. (2001) Expression cloning of a Na^+-independent aromatic amino acid transporter with structural similarity to H^+/monocarboxylate transporters. *J. Biol. Chem. 276*, 17221−17228.

(6) Halestrap, A. P. (2012) The monocarboxylate transporter family -Structure and functional characterization. *IUBMB Life 64*, 1−9.

(7) Nelissen, B., De Wachter, R., and Goffeau, A. (1997) Classification of all putative permeases and other membrane plurispanners of the major facilitator superfamily encoded by the complete genome of *Saccharomyces cerevisiae*. *FEMS Microbiol. Rev. 21*, 113−134.

(8) Brohee, S., Barriot, R., Moreau, Y., and Andre, B. (2010) YTPdb: a wiki database of yeast membrane transporters. *Biochim. Biophys. Acta 1798*, 1908−1912.

(9) van der Rest, M. E., Kamminga, A. H., Nakano, A., Anraku, Y., Poolman, B., and Konings, W. N. (1995) The plasma membrane of Saccharomyces cerevisiae: structure, function, and biogenesis. *Microbiol. Rev. 59*, 304−322.

(10) Heitman, J., Koller, A., Kunz, J., Henriquez, R., Schmidt, A., Movva, N. R., and Hall, M. N. (1993) The immunosuppressant FK506 inhibits amino acid import in *Saccharomyces cerevisiae*. *Mol. Cell. Biol. 13*, 5010−5019.

(11) Schmidt, A., Hall, M. N., and Koller, A. (1994) Two FK506 resistance-conferring genes in *Saccharomyces cerevisiae*, *TAT1* and *TAT2*, encode amino acid permeases mediating tyrosine and tryptophan uptake. *Mol. Cell. Biol. 14*, 6597−6606.

(12) Schmidt, A., Beck, T., Koller, A., Kunz, J., and Hall, M. N. (1998) The TOR nutrient signalling pathway phosphorylates NPR1 and inhibits turnover of the tryptophan permease. *EMBO J. 17*, 6924−6931.

(13) Beck, T., Schmidt, A., and Hall, M. N. (1999) Starvation induces vacuolar targeting and degradation of the tryptophan permease in yeast. *J. Cell Biol. 146*, 1227−1238.

(14) Nikko, E., and Pelham, H. R. (2009) Arrestin-mediated endocytosis of yeast plasma membrane transporters. *Traffic 10*, 1856−1867.

(15) Abe, F., and Horikoshi, K. (2000) Tryptophan permease gene *TAT2* confers high-pressure growth in *Saccharomyces cerevisiae*. *Mol. Cell. Biol. 20*, 8093−8102.

(16) Abe, F., and Iida, H. (2003) Pressure-induced differential regulation of the two tryptophan permeases Tat1 and Tat2 by ubiquitin ligase Rsp5 and its binding proteins, Bul1 and Bul2. *Mol. Cell. Biol. 23*, 7566−7584.

(17) Nagayama, A., Kato, C., and Abe, F. (2004) The *N*- and *C*-terminal mutations in tryptophan permease Tat2 confer cell growth in *Saccharomyces cerevisiae* under high-pressure and low-temperature conditions. *Extremophiles 8*, 143−149.

(18) Hiraki, T., and Abe, F. (2010) Overexpression of Sna3 stabilizes tryptophan permease Tat2, potentially competing for the WW domain of Rsp5 ubiquitin ligase with its binding protein Bul1. *FEBS Lett. 584*, 55−60.

(19) Heremans, K., and Smeller, L. (1998) Protein structure and dynamics at high pressure. *Biochim. Biophys. Acta 1386*, 353−370.

(20) Balny, C., Masson, P., and Heremans, K. (2002) High pressure effects on biological macromolecules: from structural changes to alteration of cellular processes. *Biochim. Biophys. Acta 1595*, 3−10.

(21) Abe, F. (2007) Exploration of the effects of high hydrostatic pressure on microbial growth, physiology and survival: perspectives from piezophysiology. *Biosci. Biotechnol. Biochem. 71*, 2347−2357.

(22) Gong, S., Richard, H., and Foster, J. W. (2003) YjdE (AdiC) is the arginine:agmatine antiporter essential for arginine-dependent acid resistance in *Escherichia coli*. *J. Bacteriol. 185*, 4402−4409.

(23) Iyer, R., Williams, C., and Miller, C. (2003) Arginine-agmatine antiporter in extreme acid resistance in *Escherichia coli*. *J. Bacteriol. 185*, 6556−6561.

(24) Fang, Y., Kolmakova-Partensky, L., and Miller, C. (2007) A bacterial arginine-agmatine exchange transporter involved in extreme acid resistance. *J. Biol. Chem. 282*, 176−182.

(25) Gao, X., Lu, F., Zhou, L., Dang, S., Sun, L., Li, X., Wang, J., and Shi, Y. (2009) Structure and mechanism of an amino acid antiporter. *Science 324*, 1565−1568.

(26) Fang, Y., Jayaram, H., Shane, T., Kolmakova-Partensky, L., Wu, F., Williams, C., Xiong, Y., and Miller, C. (2009) Structure of a prokaryotic virtual proton pump at 3.2 Å resolution. *Nature 460*, 1040−1043.

(27) Gao, X., Zhou, L., Jiao, X., Lu, F., Yan, C., Zeng, X., Wang, J., and Shi, Y. (2010) Mechanism of substrate recognition and transport by an amino acid antiporter. *Nature 463*, 828−832.

(28) Cirino, P. C., Mayer, K. M., and Umeno, D. (2003) Generating mutant libraries using error-prone PCR. *Methods Mol. Biol. 231*, 3−9.

(29) Gietz, R. D., and Sugino, A. (1988) New yeast-*Escherichia coli* shuttle vectors constructed with *in vitro* mutagenized yeast genes lacking six-base pair restriction sites. *Gene 74*, 527−534.

(30) Sali, A., and Blundell, T. L. (1993) Comparative protein modelling by satisfaction of spatial restraints. *J. Mol. Biol. 234*, 779−815.

(31) Lambert, C., Leonard, N., De Bolle, X., and Depiereux, E. (2002) ESyPred3D: Prediction of proteins 3D structures. *Bioinformatics 18*, 1250−1256.

(32) DeLano, W. (2002) The PyMOL Molecular Graphics System, Version 1.5.0.4, Schrödinger, LLC, http://www.pymol.org/. *The PyMOL user's manual*, DeLano Scientific, San Carlos, CA, USA.

(33) Tusnady, G. E., and Simon, I. (2001) The HMMTOP transmembrane topology prediction server. *Bioinformatics 17*, 849−850.

(34) Van Zeebroeck, G., Bonini, B. M., Versele, M., and Thevelein, J. M. (2009) Transport and signaling via the amino acid binding site of the yeast Gap1 amino acid transceptor. *Nat. Chem. Biol. 5*, 45−52.

(35) Aloy, P., Ceulemans, H., Stark, A., and Russell, R. B. (2003) The relationship between sequence and interaction divergence in proteins. *J. Mol. Biol. 332*, 989−998.
(36) Topf, M., Baker, M. L., Marti-Renom, M. A., Chiu, W., and Sali, A. (2006) Refinement of protein structures by iterative comparative modeling and CryoEM density fitting. *J. Mol. Biol. 357*, 1655−1668.
(37) Kelm, S., Shi, J., and Deane, C. M. (2010) MEDELLER: homology-based coordinate generation for membrane proteins. *Bioinformatics 26*, 2833−2840.
(38) Umebayashi, K., and Nakano, A. (2003) Ergosterol is required for targeting of tryptophan permease to the yeast plasma membrane. *J. Cell Biol. 161*, 1117−1131.
(39) Chang, S., Hu, J. P., Lin, P. Y., Jiao, X., and Tian, X. H. (2010) Substrate recognition and transport behavior analyses of amino acid antiporter with coarse-grained models. *Mol. Biosyst 6*, 2430−2438.
(40) Cox, B. G. (2013) Acids and bases: solvent effects on acid-base strength, Oxford University Press, Oxford, UK.
(41) Samyn, D. R., Ruiz-Pavon, L., Andersson, M. R., Popova, Y., Thevelein, J. M., and Persson, B. L. (2012) Mutational analysis of putative phosphate- and proton-binding sites in the *Saccharomyces cerevisiae* Pho84 phosphate:H^+ transceptor and its effect on signaling to the PKA and PHO pathways. *Biochem. J. 445*, 413−422.
(42) Abe, F. (2007) Probing for dynamics of amino acid uptake in living yeast using hydrostatic pressure. *Proceedings for the 4th International Conference on High Pressure Bioscience and Biotechnology (eds. Abe, F., and Suzuki, A.), J-STAGE 1*, 134−138.
(43) Low, P. S., and Somero, G. N. (1975) Activation volumes in enzymic catalysis: their sources and modification by low-molecular-weight solutes. *Proc. Natl. Acad. Sci. U. S. A. 72*, 3014−3018.
(44) Kunugi, S., Fukuda, M., and Ise, N. (1982) Pressure dependence of trypsin-catalyzed hydrolyses of specific substrates. *Biochim. Biophys. Acta 704*, 107−113.
(45) Makimoto, S., and Taniguchi, Y. (1987) Effect of pressure on the pre-steady-state kinetics of the hydrolysis of anilide substrates catalyzed by alpha-chymotrypsin. *Biochim. Biophys. Acta 914*, 304−307.
(46) Roche, J., Caro, J. A., Norberto, D. R., Barthe, P., Roumestand, C., Schlessman, J. L., Garcia, A. E., Garcia-Moreno, B. E., and Royer, C. A. (2012) Cavities determine the pressure unfolding of proteins. *Proc. Natl. Acad. Sci. U. S. A. 109*, 6945−6950.
(47) Lassalle, M. W., Yamada, H., Morii, H., Ogata, K., Sarai, A., and Akasaka, K. (2001) Filling a cavity dramatically increases pressure stability of the c-Myb R2 subdomain. *Proteins 45*, 96−101.
(48) Yamashita, A., Singh, S. K., Kawate, T., Jin, Y., and Gouaux, E. (2005) Crystal structure of a bacterial homologue of Na^+/Cl^--dependent neurotransmitter transporters. *Nature 437*, 215−223.
(49) Krishnamurthy, H., and Gouaux, E. (2012) X-ray structures of LeuT in substrate-free outward-open and apo inward-open states. *Nature 481*, 469−474.
(50) Piscitelli, C. L., and Gouaux, E. (2012) Insights into transport mechanism from LeuT engineered to transport tryptophan. *EMBO J. 31*, 228−235.
(51) Merhi, A., Gerard, N., Lauwers, E., Prevost, M., and Andre, B. (2011) Systematic mutational analysis of the intracellular regions of yeast Gap1 permease. *PLoS One 6*, e18457.
(52) Huang, Y., Lemieux, M. J., Song, J., Auer, M., and Wang, D. N. (2003) Structure and mechanism of the glycerol-3-phosphate transporter from *Escherichia coli*. *Science 301*, 616−620.
(53) Soares-Silva, I., Sa-Pessoa, J., Myrianthopoulos, V., Mikros, E., Casal, M., and Diallinas, G. (2011) A substrate translocation trajectory in a cytoplasm-facing topological model of the monocarboxylate/H^+ symporter Jen1p. *Mol. Microbiol. 81*, 805−817.
(54) Simossis, V. A., and Heringa, J. (2005) PRALINE: a multiple sequence alignment toolbox that integrates homology-extended and secondary structure information. *Nucleic Acids Res. 33*, W289−94.